

Next generation long baseline experiments on the path to leptonic CP violation

P. Migliozzi^{a,1} and F. Terranova^{b,2}

^a I.N.F.N., Sezione di Napoli, Naples, Italy

^b I.N.F.N., Laboratori Nazionali di Frascati, Frascati (Rome), Italy

Abstract

In this paper we quantify the trade-off between setups optimized to be ancillary to Phase II Superbeams or Neutrino Factories and experiments tuned for maximal sensitivity to the subdominant terms of the neutrino transition probability at the atmospheric scale (“maximum discovery potential”). In particular, the θ_{13} sensitivity is computed for both Phase I superbeams (JHF-SK and NuMI Off-Axis) and next generation long baseline experiments (ICARUS, OPERA and MINOS). It is shown that Phase I experiments cannot reach a sensitivity able to ground (or discourage in a definitive manner) the building of Phase II projects and that, in case of null result and without a dedicated $\bar{\nu}$ run, this capability is almost saturated by high energy beams like CNGS, especially for high values of the ratio $\Delta m_{21}^2/|\Delta m_{31}^2|$.

PACS: 14.60.Pq, 14.60.Lm

¹pasquale.migliozzi@cern.ch

²francesco.terranova@cern.ch

1 Introduction

The possibility to perform a CKM-like precision physics in the leptonic sector employing terrestrial neutrino oscillation experiments has been deeply debated in the last few years. At present, the occurrence of neutrino oscillations seems rather well established [1, 2, 3]. Current experimental evidence indicates two hierarchical mass scale differences ($\Delta m_{21}^2 \ll |\Delta m_{32}^2| \simeq |\Delta m_{31}^2|$) driving, respectively, the oscillations at the “solar” and “atmospheric” scale. Moreover, the $\alpha \equiv \Delta m_{21}^2/|\Delta m_{31}^2|$ ratio is constrained by the LMA solution of the solar neutrino puzzle to lie between $\mathcal{O}(0.1)$ and $\mathcal{O}(0.01)$ [4]. If this scenario will be confirmed after the completion of ongoing experiments (K2K [2], KAMLAND [3] and MiniBoone [5]) and next generation long baseline projects (MINOS [6], ICARUS [7], OPERA [8]), terrestrial neutrino experiments based on “Superbeams” (SB) or “Neutrino Factories” (NF) could be the ideal tool for precision measurements of the PMNS [9] leptonic mixing matrix and the discovery of leptonic CP violation [10]. These experiments explore subdominant effects in the neutrino transition probabilities at the atmospheric scale which, in general, are suppressed by at least one power of α . Hence, the recent KAMLAND result places SB and NF proposals on a firmer ground since guarantees that subdominant effects will not be suppressed to an unobservable level ($\alpha \ll 10^{-2}$). This condition, however, is not enough to establish the physics reach of SB/NF. As for the case of CKM physics, CP violating effects depend on the size of the Jarlskog invariant [11]. In the standard parameterization [12] of the PMNS matrix this coefficient can be expressed as:

$$J \equiv s_{12}s_{23}s_{13}c_{12}c_{23}c_{13}^2 \sin \delta = \frac{1}{8} \sin 2\theta_{12} \sin 2\theta_{23} \sin 2\theta_{13} c_{13} \sin \delta \quad (1)$$

where $s_{ij} \equiv \sin \theta_{ij}$ and $c_{ij} \equiv \cos \theta_{ij}$. Differently from the quark case, the leptonic Jarlskog invariant is enhanced by the large mixing angles θ_{23} and θ_{12} . On the other hand, due to the null result of the CHOOZ [13] and PALO VERDE [14] experiments, the full three-flavor mixing of neutrinos is still unestablished and only upper limits on the $\sin^2 2\theta_{13}$ parameter have been drawn ($\sin^2 2\theta_{13} < \mathcal{O}(10^{-1})$). Moreover, no theoretical inputs are available to constrain the size of θ_{13} in a convincing manner, so that its experimental determination is mandatory. The discovery of $\theta_{13} \neq 0$ has not only a scientific relevance but also a high practical value. The commissioning and running of an apparatus to observe CP violation in the leptonic sector at the atmospheric scale (e.g. JHF-Phase II or a Neutrino Factory) is a major technical and economical challenge; since most of its physics reach - in particular the measurement of leptonic CP violation and the determination of U_{e3} in the PMNS matrix - depends crucially on the size of θ_{13} , the latter should be determined by “Phase I” experiments (e.g. JHF-SK [15] or NuMI Off-Axis [16]) tuned to maximize their θ_{13} sensitivity. Otherwise, the physics case of SB/NF should be drawn independently of their PMNS reach. This is marginally possible for JHF-Phase II (proton decay with HyperK) but rather unrealistic for NF. The physics case of Phase I experiments is very appealing due to their

unprecedented precision in the determination of the parameters leading the oscillations at the atmospheric scale (θ_{23} and $|\Delta m_{31}^2|$) and their significant discovery potential for high values of θ_{13} . On the other hand, the sensitivity of Phase I experiments to θ_{13} has been questioned since a significant deterioration is expected once we account for our complete ignorance of the leptonic CP phase, the sign of Δm_{31}^2 and the θ_{23} ambiguity [17, 18]. In this context, the advantage of a “pure” θ_{13} measurement has been put forward especially in connection with new reactor experiments [19].

In this letter we quantify the trade-off between a setup optimized to be ancillary with respect the SB/NF project (maximum θ_{13} sensitivity) and one highly sensitive to the subdominant terms of the transition probability (maximum discovery potential). In particular, we challenge the claim that a Phase I experiment can reach a sensitivity able to ground (or discourage in a definitive manner) the building of SB/NF and show that, in case of null results and without a dedicated $\bar{\nu}$ run, this capability is almost saturated by first generation long baseline experiments like CNGS.

2 Oscillation probabilities

The next generation long baseline experiments (MINOS, ICARUS and OPERA) and Phase I experiments (JHF-SK and NuMI Off-Axis) employ baselines in the 300-700 km range. In most of the cases, the neutrino energy is optimized to maximize the oscillation probability at the atmospheric scale for the corresponding baseline ($\langle E_\nu \rangle \simeq 0.7 - 3$ GeV). The CNGS experiments, however, make use of a high energy beam, well beyond the kinematic threshold for τ production ($\langle E_\nu \rangle \simeq 17$ GeV). The main parameters for the setups under consideration are listed in Table 1. In all cases the subleading oscillations at the solar scale are suppressed by at least one order of magnitude compared with the atmospheric ones. Hence, oscillation probabilities can be expanded in the small parameters α and $\sin 2\theta_{13}$. The inclusion of matter effects is simplified here, since the earth density can be considered constant along baselines shorter than ~ 1000 km. In particular, the $\nu_\mu \rightarrow \nu_e$ oscillation probability can be expressed as [20, 21]:

$$\begin{aligned}
P_{\nu_\mu \rightarrow \nu_e} &\simeq \sin^2 2\theta_{13} \sin^2 \theta_{23} \frac{\sin^2[(1 - \hat{A})\Delta]}{(1 - \hat{A})^2} \\
&- \alpha \sin 2\theta_{13} \xi \sin \delta \sin(\Delta) \frac{\sin(\hat{A}\Delta)}{\hat{A}} \frac{\sin[(1 - \hat{A})\Delta]}{(1 - \hat{A})} \\
&+ \alpha \sin 2\theta_{13} \xi \cos \delta \cos(\Delta) \frac{\sin(\hat{A}\Delta)}{\hat{A}} \frac{\sin[(1 - \hat{A})\Delta]}{(1 - \hat{A})} \\
&+ \alpha^2 \cos^2 \theta_{23} \sin^2 2\theta_{12} \frac{\sin^2(\hat{A}\Delta)}{\hat{A}^2}
\end{aligned}$$

$$\equiv O_1 + O_2(\delta) + O_3(\delta) + O_4 . \quad (2)$$

In this formula $\Delta \equiv \Delta m_{31}^2 L / (4E)$ and the terms contributing to the Jarlskog invariant are split into the small parameter $\sin 2\theta_{13}$, the $\mathcal{O}(1)$ term $\xi \equiv \cos \theta_{13} \sin 2\theta_{12} \sin 2\theta_{23}$ and the CP term $\sin \delta$; $\hat{A} \equiv 2\sqrt{2}G_F n_e E / \Delta m_{31}^2$ with G_F the Fermi coupling constant and n_e the electron density in matter. Note that the sign of \hat{A} depends on the sign of Δm_{31}^2 which is positive (negative) for normal (inverted) hierarchy of neutrino masses. The dominant contributions among the four terms $O_1 \dots O_4$ of Eq. 2 are determined by the choice of L and E . In the following, if not stated explicitly, we assume the present best fits for the solar and atmospheric parameters ($\Delta m_{21}^2 = 7.3 \times 10^{-5} \text{ eV}^2$, $\sin^2 2\theta_{12} = 0.8$, $\Delta m_{31}^2 = 2.5 \times 10^{-3} \text{ eV}^2$, $\sin^2 2\theta_{23} = 1$) [4]³.

	JHF-SK	NuMI-OA	MINOS	ICARUS	OPERA
Baseline (km)	295	712	735	732	732
Mean energy (GeV)	0.76	2.22	3	17	17
Exposure (kton×years)	22.5×5	17×5	5.4×2	2.4×5	1.7×5
L/E (km/GeV)	388	321	245	43	43

Table 1: Main parameters of the Phase I and long baseline experiments.

JHF-SK

JHF-SK has been tuned to maximize the discovery potential and subdominant contributions depending on the CP phase are enhanced. Given its short baseline matter effects represent a small correction to the oscillation probability ($\hat{A} \simeq 5 \times 10^{-2}$). Assuming an average neutrino energy of 0.76 GeV, the following hierarchy among the terms of Eq. 2 is obtained:

$$P_{\nu_\mu \rightarrow \nu_e} \simeq \sin^2 2\theta_{13} A_1 - \sin \delta \sin 2\theta_{13} \alpha A_2 + \cos \delta \sin 2\theta_{13} \alpha \cos(\Delta) A_3 + \alpha^2 A_4 \quad (3)$$

where the A_i ($i = 1, \dots, 4$) coefficients are $\mathcal{O}(1)$. The actual values of the terms contributing to Eq. 2 are shown in Fig. 1. Here, the δ -depending terms O_2 and O_3 are computed at maximum amplitude, $O_2 = O_2(\delta = -\pi/2)$ and $O_3 = O_3(\delta = 0)$, to illustrate the impact of assuming complete ignorance on δ in the extraction of $\sin^2 2\theta_{13}$. Of course, in the oscillation probability formula when O_2 (O_3) is maximal, i.e. $\delta = -\pi/2$ ($\delta = 0$), the other coefficient O_3 (O_2) is zero. For $\sin^2 2\theta_{13}$ sufficiently high:

$$P_{\nu_\mu \rightarrow \nu_e} \simeq \sin 2\theta_{13} (\sin 2\theta_{13} A_1 - \sin \delta \alpha A_2) \quad (4)$$

³For $\theta_{23} \neq \pi/4$ other degenerate solutions appear at $\theta'_{23} = \pi/2 - \theta_{23}$ [22].

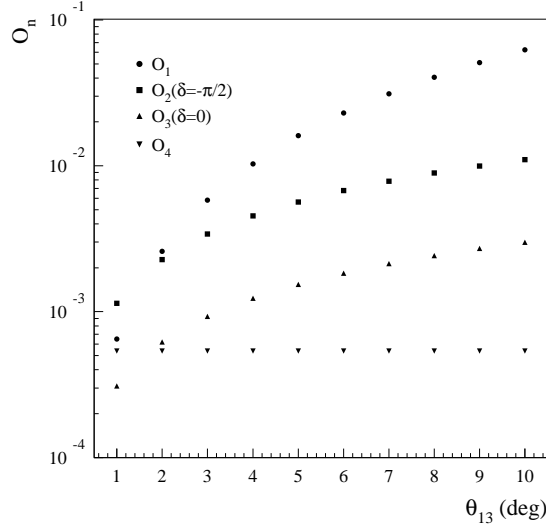


Figure 1: Contribution of the $O_1 \dots O_4$ terms to the oscillation probability in the JHF-SK scenario.

Eq. 3 and 4 show that the deterioration of the $\sin^2 2\theta_{13}$ sensitivity coming from the θ_{13} - δ ambiguity [23] is strictly connected to the mass scale ratio α . Hence, the maximum sensitivity is achieved in the limit $\alpha \rightarrow 0$ which corresponds to minimum sensitivity to the subdominant terms of $P_{\nu_\mu \rightarrow \nu_e}$ (minimum discovery potential). Clearly, this contradictory request is at the origin of the conflict between setups ancillary to SB/NF and experiments able to explore a significant fraction of the PMNS parameter space. For JHF-SK, the deterioration effect becomes sizable already at $\theta_{13} \sim 3^\circ$ (see Fig. 1). Values of α higher than the ones assumed in Fig. 1 ($\alpha \simeq 0.03$) imply earlier appearance of the $(\theta_{13} - \delta)$ deterioration effect.

Note that Eq. 3 cannot be used in a straightforward manner to extract the actual sensitivity of a Phase I experiment. The signal rate is:

$$S \equiv Y A \int dE \Phi(E) P_{\nu_\mu \rightarrow \nu_e}(E) \sigma(E) \epsilon(E) \quad (5)$$

where $\Phi(E)$ is the ν_μ flux at the surface of the detector, A is proportional to the detector mass, Y are the years of data taking and $\sigma(E) \cdot \epsilon(E)$ is the production cross-section weighted with the detection efficiency for the ν_e CC final state. The signal rate is proportional to $P_{\nu_\mu \rightarrow \nu_e}(\langle E \rangle)$ only in the narrow band limit $\Phi(E) \rightarrow \delta(E - \langle E \rangle)$. The minimum accessible probability P_{min} depends on the background rate and it has to be computed through a full simulation. We further address this issue in Sec. 3. Finally, note that for P_{min} sufficiently low (“Phase II” measurements), setups can be envisaged to lift explicitly the $\theta_{13} - \delta$ ambiguity, e.g. combining different baselines [24] or different oscillation channels [25] or building a single baseline experiment with a

detector capable of observing more than one oscillation peak [26].

NuMI Off-Axis and MINOS

The NuMI Off-Axis proposal envisages the possibility of getting a very narrow ν_μ beam placing a dedicated detector for ν_e appearance (20 kton, low-Z calorimeter) at an angle of $\sim 0.7^\circ$ with respect to the present NuMI axis. Again, L and E are tuned close to the first oscillation maximum at the atmospheric scale. A significant reduction of the background coming from ν_μ NC with π^0 production can be reached, compared with the MINOS setup, thanks to the suppression of the high energy tail of the ν_μ beam. Once more, the terms contributing to Eq. 2 keeps the form of Eq. 3 with A_i ($i = 1, \dots, 4$) ranging between 0.4 and 0.6. However, both MINOS and NuMI Off-Axis employ a baseline of $\simeq 700$ km and matter effects are sizable ($\hat{A} \simeq 0.2$) in this regime since they modify the size of the leading term A_1 . As a consequence, these setups offer a significant sensitivity to the sign of Δm_{31}^2 . On the other hand, if it is not possible to disentangle the $\text{sign}(\Delta m_{31}^2)$ degeneracy from the effect proportional to $\sin^2 2\theta_{13}$, an additional source of deterioration of the $\sin^2 2\theta_{13}$ sensitivity appears. In principle, it could be possible to re-tune NuMI Off-Axis releasing the condition $\Delta \simeq \pi/2$ and, hence, modifying the relative weights of the A_i coefficients. In this scenario, NuMI would be complementary to JHF-SK since the former would lower its bare $\sin^2 2\theta_{13}$ sensitivity allowing the latter to relieve the $(\delta - \theta_{13})$ deterioration discussed above. This possibility and the overall improvement in the PMNS reach of the synergic JHF/NuMI physics programme has been discussed in details in [17, 19] and will not be further considered here.

CNGS

The CNGS beam has been tuned to reach maximum sensitivity to the ν_τ appearance channel. To overcome the limitation of the high threshold for τ production, the condition $\Delta \simeq \pi/2$ has been given up and $\Delta_{CNGS} \simeq \mathcal{O}(10^{-1})$. As a consequence, the oscillation probability is suppressed by the dumping term $\Delta^2 \simeq \mathcal{O}(10^{-2})$

$$P(\nu_\mu \rightarrow \nu_\tau) \simeq \cos^4 \theta_{13} \sin^2 2\theta_{23} \Delta^2 \quad (6)$$

but the event rate profits of the high ν_τ -CC cross-section. The same dumping factor limits the search for $\nu_\mu \rightarrow \nu_e$. Again, this loss of signal events is partially compensated by the linear rise of the ν_e -CC cross-section and by the high granularity of the corresponding detectors tuned for ν_τ (in particular $\tau \rightarrow e$) appearance and hence, extremely effective in suppressing the NC(π^0) and $\nu_\mu \rightarrow \nu_\tau \rightarrow \tau(\rightarrow e)X$ background. It has been shown [27] that ICARUS and OPERA combined could explore the region down to $\sin^2 2\theta_{13} \sim 0.025$ at $|\Delta m_{31}^2| = 2.5 \times 10^{-3} \text{ eV}^2$ and assuming 6.75×10^{19} pot/year

($\sin^2 2\theta_{13} < 0.03$ for ICARUS and $\sin^2 2\theta_{13} < 0.05$ for OPERA separately). The analysis is dominated by the statistical fluctuations of the ν_e beam contamination from K_{e3} decays and, for higher exposure time, by the systematics uncertainty on its overall normalization⁴ (see Fig. 7 in Section 3). However, this analysis does not include the deterioration effect coming from the CP phase and the sign of Δm_{31}^2 . In principle, matter effects should be even higher than NuMI because \hat{A} grows linearly with E and the two setups have the same baseline ($\hat{A} \simeq 1.6$). However, since $|(1 - \hat{A})\Delta| \ll 1$, we get:

$$\frac{\sin^2[(1 - \hat{A})\Delta]}{(1 - \hat{A})^2} \simeq \Delta^2 \quad (7)$$

and the leading term A_1 turns out to be unaffected by the sign of Δm_{31}^2 . Eq. 2 reads now:

$$P_{\nu_\mu \rightarrow \nu_e} \simeq \left[\sin^2 2\theta_{13} A_1 - \sin \delta \sin 2\theta_{13} \alpha \Delta A_2 + \cos \delta \sin 2\theta_{13} \alpha A_3 + \alpha^2 A_4 \right] \Delta^2 \quad (8)$$

and, again, $A_1 \dots A_4$ are $\mathcal{O}(1)$ coefficients, albeit different from the ones of Eq. 3. The values of the terms contributing to Eq. 2 at CNGS are shown in Fig. 2. The overall scale is suppressed by Δ^2 and the role of the O_2 and O_3 terms are exchanged w.r.t. JHF due to the different size of $\sin \Delta$ and $\cos \Delta$. Here, O_3 is responsible for the $(\delta - \theta_{13})$ deterioration effect which is sizable in the same θ_{13} region as for JHF. Note, however, that O_3 (O_2) is odd (even) under the transformation $\Delta m_{31}^2 \rightarrow -\Delta m_{31}^2$; so, at CNGS, going from normal to inverted hierarchy has the same effect of performing a $\delta \rightarrow \pi - \delta$ transformation in the CP phase. Note also that both JHF-SK and CNGS see a deterioration of their sensitivity to θ_{13} starting from the 3° region (or before for higher α).

3 Numerical calculations

Analyses of the $\nu_\mu \rightarrow \nu_e$ channel in the leading order approximation $P(\nu_\mu \rightarrow \nu_e) \simeq O_1$ have been published by the collaborations involved in the Phase I and next generation long baseline experiments. Hence, it is possible to make a reliable estimation of the actual sensitivities side-stepping the full simulation of the various setups. The condition that excludes a point $(\sin^2 2\theta_{13}, \Delta m_{31}^2)$ of the parameter space at a given confidence level, once the null hypothesis $\sin^2 2\theta_{13} = 0$ has been experimentally observed and a given value of δ is assumed, is

$$\chi^2(\sin^2 2\theta_{13}, \Delta m_{31}^2) > \zeta \quad (9)$$

⁴The CNGS physics programme does not foresee the construction of a near detector.

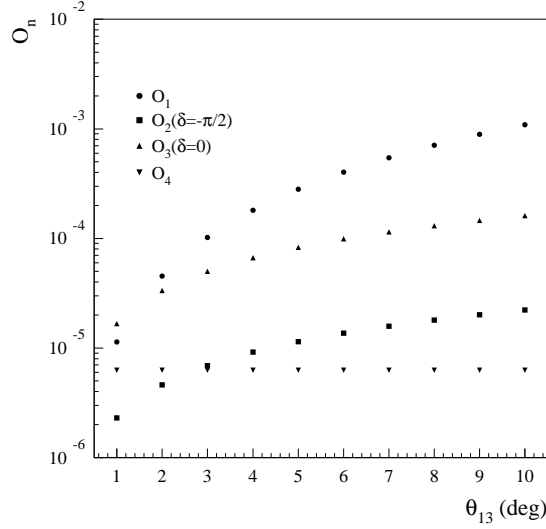


Figure 2: Contribution of the $O_1 \dots O_4$ terms to the oscillation probability at CNGS.

where

$$\chi^2(\sin^2 2\theta_{13}, \Delta m_{31}^2) \equiv \left(\frac{R^{th} - R^{obs}}{\sigma} \right)^2 = \frac{[(S(\sin^2 2\theta_{13}, \Delta m_{31}^2) + B) - (S_{null} + B)]^2}{S_{null} + B + \eta^2 B^2} > \zeta \quad (10)$$

In this formula, which holds in Gaussian approximation, R^{th} is the expected ν_e rate for the current value of $(\sin^2 2\theta_{13}, \Delta m_{31}^2)$ and R^{obs} is the rate corresponding to the null hypothesis. Eq. 2 shows that the null hypothesis is independent of the CP phase and the sign of Δm_{31}^2 and depends only on $|\Delta m_{31}^2|$. S and B represent the signal and background rate, η is the systematic uncertainty on the background normalization and ζ is a constant depending on the confidence level ($\zeta = 4.6$ for 90% CL contours). If the $\tau \rightarrow e$ contamination is negligible w.r.t. the $\text{NC}(\pi^0)$ and the ν_e contamination from the beam in the Δm_{31}^2 region of interest, B is independent of the oscillation parameters. Dropping the Δm_{31}^2 dependence, the minimum value of $\sin^2 2\theta_{13}$ excluded by the experiment is the one fulfilling:

$$\frac{[(S(\sin^2 2\theta_{13}) + B) - (S_{null} + B)]^2}{S_{null} + B + \eta^2 B^2} = \zeta \quad (11)$$

The expected signal rate in Eq. 10 can be written (see Eq. 5) as:

$$S(\sin^2 2\theta_{13}, \delta) \equiv Y A \int dE \Phi(E) P_{\nu_\mu \rightarrow \nu_e}(\sin^2 2\theta_{13}, \delta, E) \sigma(E) \epsilon(E) \quad (12)$$

and in the narrow beam approximation ($\bar{E} \equiv \langle E \rangle$)

$$S(\sin^2 2\theta_{13}, \delta) = Y \gamma P_{\nu_\mu \rightarrow \nu_e}(\sin^2 2\theta_{13}, \delta, \bar{E}) \quad (13)$$

where

$$\gamma \equiv A \Phi(\bar{E}) \sigma(\bar{E}) \epsilon(\bar{E}) \quad (14)$$

Similarly, $S_{null} = Y \gamma P_{\nu_\mu \rightarrow \nu_e}(\sin^2 2\theta_{13} = 0, \bar{E}) \equiv Y \gamma P_{null}(\bar{E})$ and $B \equiv Y \beta$, being β the background rate per year. Now Eq. 10 reads:

$$\begin{aligned} P(\sin^2 2\theta_{13}, \delta, \bar{E}) &> P_{null}(\bar{E}) + \sqrt{\zeta} \left\{ \frac{\beta}{Y \gamma^2} + \frac{\eta^2 \beta^2}{\gamma^2} + \frac{P_{null}(\bar{E})}{Y \gamma} \right\}^{1/2} \simeq \\ &P_{null}(\bar{E}) + \sqrt{\zeta} \left\{ \frac{\beta}{Y \gamma^2} + \frac{\eta^2 \beta^2}{\gamma^2} \right\}^{1/2} \end{aligned} \quad (15)$$

Exclusion plots for $\sin^2 2\theta_{13}$ are available [7, 15, 16, 27, 28] in the approximation $P(\nu_\mu \rightarrow \nu_e) \simeq O_1$. This corresponds to the assumption $\delta = 0$ for on-peak experiment ($\Delta \simeq \pi/2$) and $\delta = \pi/2$ for off-peak ones ($\Delta \ll \pi/2$). Hence, it is possible to extract the minimum accessible probability P_{min} :

$$P_{min} \equiv \sqrt{\zeta} \left\{ \frac{\beta}{Y \gamma^2} + \frac{\eta^2 \beta^2}{\gamma^2} \right\}^{1/2} \quad (16)$$

from literature and compute Eq. 15 using the correct oscillation probability⁵. Fig. 3 shows the $\sin^2 2\theta_{13}$ sensitivity at 90% CL as a function of δ for JHF-SK and CNGS. Note that for positive values of the CP phase, the δ dependence of JHF-SK has the worst possible behaviour for a Phase I experiment, since the minimum sensitivity to $\sin^2 2\theta_{13}$ is achieved at maximum CP violation (maximum discovery potential of phase II setups). This is illustrated in Fig.4. Plot (a) shows the region where a 3σ discovery of CP violation at JHF-HK can be achieved as a function of $\sin \delta$ and $\sin^2 2\theta_{13}$ [29]. The horizontal band is the exclusion limit of JHF-SK at 90%CL in the approximation $P(\nu_\mu \rightarrow \nu_e) \simeq O_1$. The correct exclusion limit from JHF-SK is shown in plot (b) for positive (dashed line) or negative (dotted line) Δm_{31}^2 . Assuming complete ignorance on the value of the CP phase and using no other external information to lift the $\theta_{13} - \delta$ ambiguity (e.g. an $\bar{\nu}$ run with similar statistics), the actual excluded $\sin^2 2\theta_{13}$ is

⁵The results shown in this sections have been obtained using the complete three family oscillation formula at constant matter density and not the approximate expansion of Eq. 2.

$$\sin^2 2\theta_{13}\Big|_{excl} = \max_{-\pi < \delta < \pi} \sin^2 2\theta_{13}\Big|_{excl}(\delta) \quad (17)$$

In other words, the effective sensitivity is computed “finding the largest value of $\sin^2 2\theta_{13}$ which fits the true $\sin^2 2\theta_{13} = 0$ at the selected confidence level” [17]. If we assume complete ignorance also on the sign of Δm_{31}^2 the final excluded value of $\sin^2 2\theta_{13}$ is the maximum between the value of $\sin^2 2\theta_{13}$ calculated by Eq. 17 assuming $\Delta m_{31}^2 > 0$ and the one with $\Delta m_{31}^2 < 0$.

Fig. 5 shows the expected precision for the experiments considered in Sec. 2 for $|\Delta m_{31}^2| = 3 \cdot 10^{-3} \text{ eV}^2$ and $\Delta m_{21}^2 = 7.3 \cdot 10^{-5} \text{ eV}^2$. The empty boxes indicate the deterioration coming from the integration on the CP phase δ . Full boxes show the effect of the $\text{sign}(\Delta m_{31}^2)$ degeneracy. A few comments are in order. Both JHF-SK and CNGS appear to be almost insensitive to the sign of Δm_{31}^2 but in fact the effect is subtler. In JHF-SK, the leading term O_1 is independent of the transformation $\Delta m_{31}^2 \rightarrow -\Delta m_{31}^2$ thanks to the smallness of the \hat{A} parameter. O_2 is invariant under this transformation and O_3 is suppressed as well as O_4 . On the other hand, at CNGS the leading term O_1 does not depend significantly on the Δm_{31}^2 sign thanks to the cancellation of matter effect at work for small values of $|(1 - \hat{A})\Delta|$ (see Sec. 2). The next-to-leading term in the oscillation probability (O_3) is odd under the sign exchange. This effect is equivalent to a $\delta \rightarrow \pi - \delta$ transformation so that the same variation of probability appears during the integration in δ ; hence, in Fig. 5 the deterioration of the sensitivity coming from the sign degeneracy is absorbed into the deterioration caused by the CP phase. This different behavior is unveiled examining the exclusion plots at different values of δ (Fig. 3) ⁶. On the other hands, MINOS and NuMI Off-Axis have the highest sensitivity to the $\Delta m_{31}^2 \rightarrow -\Delta m_{31}^2$ transformation since the condition $\hat{A} \neq 0$ affects directly the leading term O_1 . Plots similar to Fig. 5 have already been obtained for JHF and NuMI Off-Axis by the authors of [17] using a detailed simulation of the setups. The bands of Fig. 5 corresponding to these experiments are in good agreement with their results. The CNGS sensitivity has been cross-checked applying the full oscillation probability to the analysis described in [27]. The sensitivity deterioration at $|\Delta m_{31}^2| = 3 \cdot 10^{-3} \text{ eV}^2$ for the two experiments separately is $0.025 \rightarrow 0.034$ (ICARUS) and $0.035 \rightarrow 0.045$ (OPERA).

In Sec. 2 we argued that the trade-off between maximal $\sin^2 2\theta_{13}$ sensitivity and maximal PMNS reach is connected with the size of the ratio $\alpha \equiv \Delta m_{21}^2 / |\Delta m_{31}^2|$. Fig. 6 shows the $\sin^2 2\theta_{13}$ sensitivity versus α for mass ratios up to 10^{-1} . As expected, the Phase I experiments loose their capability to perform a “pure” $\sin^2 2\theta_{13}$ measurement in the high-LMA region of Δm_{21}^2 . Note also that the present CHOOZ limits become more stringent in the high- Δm_{21}^2 regime [30].

Fig. 7-a describes the sensitivity in $\sin^2 2\theta_{13}$ versus the integrated flux expressed

⁶Note that for values of $\sin^2 2\theta_{13}$ close to the CHOOZ limit, it could be possible to use synergically JHF-SK and CNGS to get information on the hierarchy of neutrino masses.

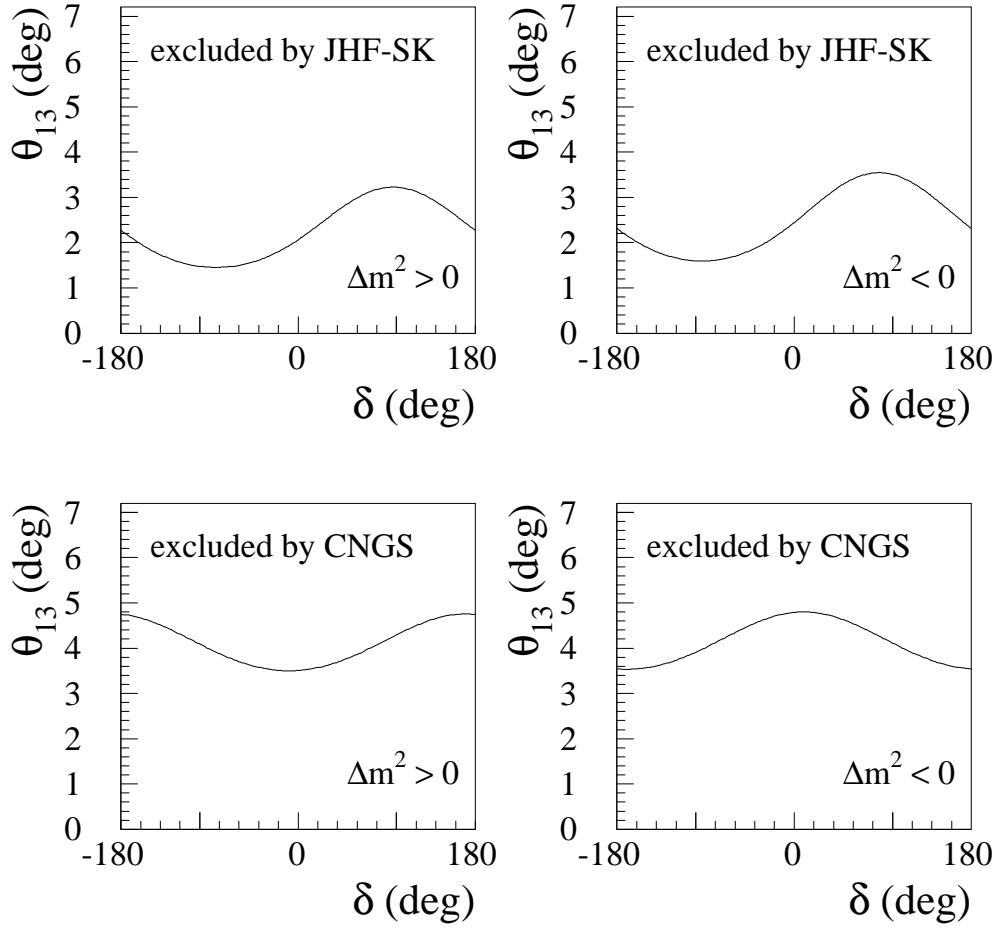


Figure 3: $\sin^2 2\theta_{13}$ sensitivity at 90% CL versus δ

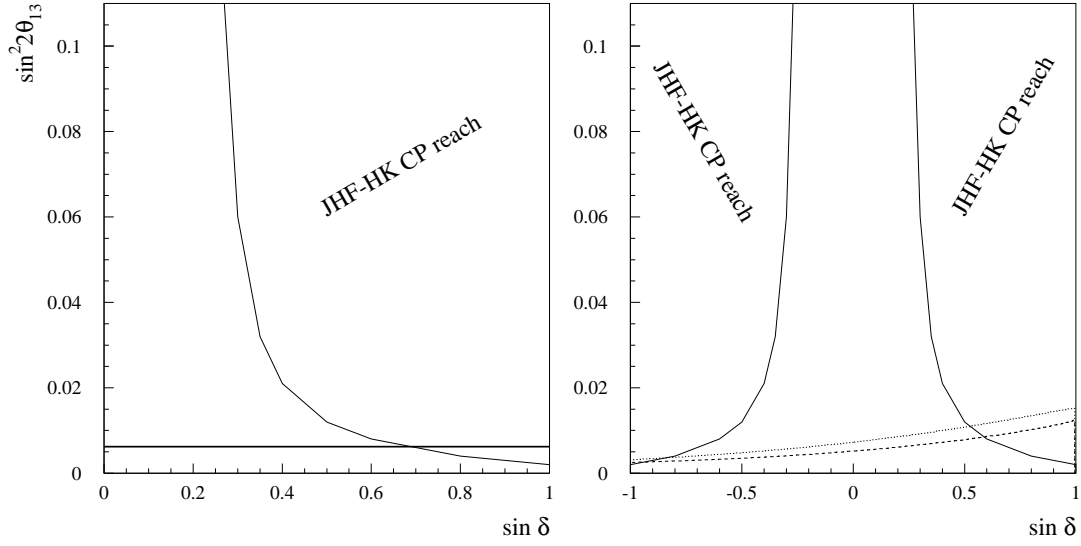


Figure 4: Sensitivity to CP violation (3σ discovery) of JHF-HK as a function of $\sin \delta$ and $\sin^2 2\theta_{13}$. The horizontal band in (a) represent the value excluded by JHF-SK at 90% CL assuming $P(\nu_\mu \rightarrow \nu_e) \simeq O_1$. The corresponding exclusion region for the full oscillation probability is shown in (b) for positive (dashed line) or negative (dotted line) Δm_{31}^2 .

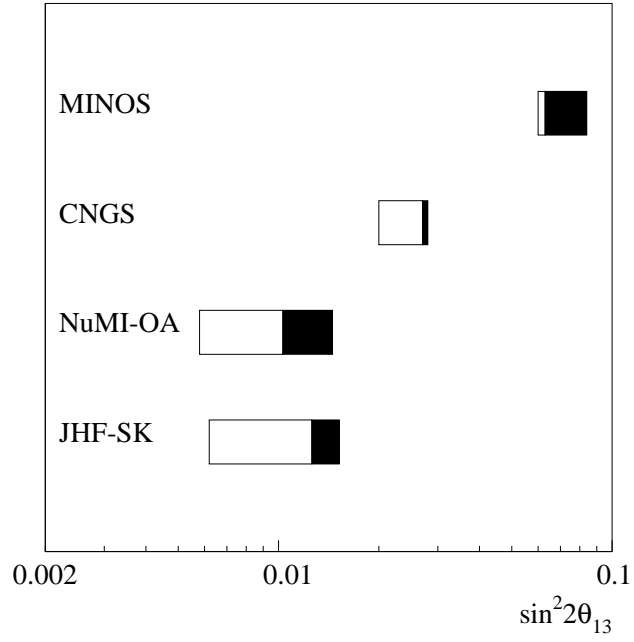


Figure 5: $\sin^2 2\theta_{13}$ sensitivity at 90% CL. Empty boxes correspond to the deterioration due to the ignorance on the δ phase. Full boxes indicate further deterioration coming from the sign of Δm_{31}^2 .

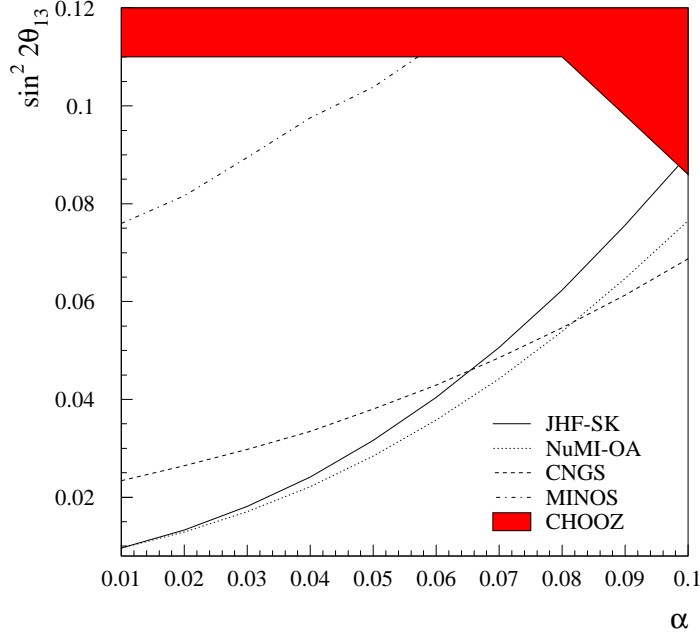


Figure 6: $\sin^2 2\theta_{13}$ sensitivity at 90% CL versus $\alpha \equiv \Delta m^2_{21}/|\Delta m^2_{31}|$

in years of data taking, assuming the nominal intensity of JHF-SK ⁷. The limits have been extracted rescaling naively with \sqrt{Y} the minimum accessible probability P_{min} and ignoring the saturation effect coming from the background normalization. In fact, JHF is expected to be limited by systematics only in the Phase II of its physics programme. It is worth noting that the deterioration coming from the degeneracies does not imply a plateau of the sensitivity. Phase II experiments will access a region of $\sin^2 2\theta_{13}$ deeper than the one accessible by their Phase I counterparts. As an example in Fig. 7-a the achievable sensitivity on $\sin^2 2\theta_{13}$ after one year data taking of JHF-HK is shown ($\Delta m^2_{21} = 7.3 \times 10^{-5} \text{ eV}^2$).

After the $\bar{\nu}$ run, JHF-HK will be able to observe maximal CP violation in the leptonic sector down to $\sin^2 2\theta_{13} \sim 2 \times 10^{-3}$ for $\Delta m^2_{21} \sim 5 \times 10^{-5} \text{ eV}^2$ [31] and the highest the solar mass, the better the CP-sensitivity (the worse the Phase I “pure” $\sin^2 2\theta_{13}$ sensitivity). So, a null result of JHF-SK cannot rule out convincingly the possibility to perform PMNS precision physics with terrestrial experiments. Of course, this holds also for the Neutrino Factories which have an even higher CP sensitivity than JHF-HK.

Finally, Fig. 7-b shows the $\sin^2 2\theta_{13}$ sensitivity versus the exposure for a CNGS-like

⁷It corresponds to a proton intensity of 0.7 MW. Note that 1 year of JHF-HK data taking corresponds to about 125 years of JHF-SK due to the increase of beam intensity and detector mass.

beam. For the actual CNGS, the background systematics η cannot be neglected. The horizontal lines in the plot indicate the region where the beam systematics will saturate the limits on $\sin^2 2\theta_{13}$ ($\sqrt{B} = \eta B$). They correspond to a precision in the normalization of the ν_e background of 10% and 5%. The limit from beam systematics for a setup with a near detector ($\eta \simeq 2\%$) is also shown.

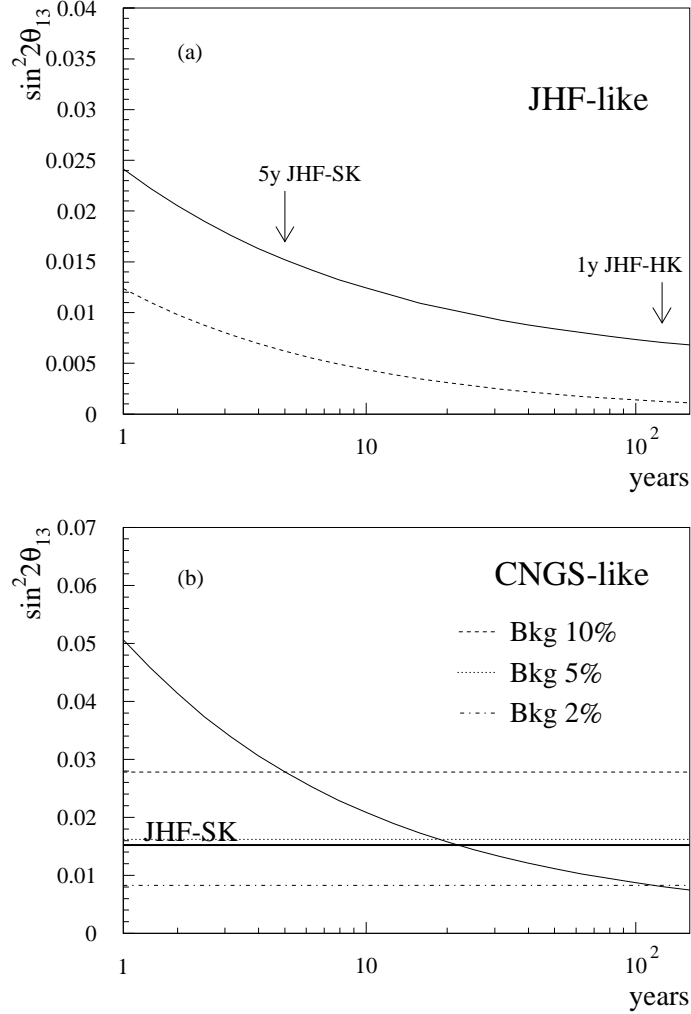


Figure 7: $\sin^2 2\theta_{13}$ sensitivity at 90% CL versus years of exposures for JHF (a) and CNGS (b). In (a) the solid line represents the sensitivity keeping into account the CP phase and $\text{sign}(\Delta m_{31}^2)$ deterioration. The dashed line shows the expected sensitivity assuming $P(\nu_\mu \rightarrow \nu_e) = O_1$. In (b) the horizontal lines indicate the region where the $\sin^2 2\theta_{13}$ sensitivity becomes limited by the beam systematics (see text).

Up to now, we only considered the interplay between on-peak and off-peak beams

in the case of null result. However, for high values of θ_{13} ($\theta_{13} \gtrsim 7^\circ$) CNGS could be able to establish $\nu_\mu \rightarrow \nu_e$ oscillations at 3σ level for any value of δ . In this scenario, a very strong improvement in the measurement of the angle (as a function of δ) is obtained after the JHF-SK data taking. The three plots on the left of Fig. 8 show the 90% CL allowed region after 5 years of CNGS data taking for $\theta_{13} = 10^\circ$, normal hierarchy and $\delta = -90^\circ$ (upper), $\delta = 0^\circ$ (middle), $\delta = 90^\circ$ (lower plot). The plots on the right show the corresponding regions obtained combining CNGS data with a 5-year run of JHF-SK. Note that the combined (θ_{13}, δ) band has no more uniform width, as it would be for JHF-SK alone, and shrinking of the region around $\delta = \pm 90^\circ$ results from the combination of experiments with different (θ_{13}, δ) patterns. Clearly, it is possible to lift explicitly the (θ_{13}, δ) correlation after a $\bar{\nu}$ run. For the optimization of the JHF-SK $\nu + \bar{\nu}$ data taking in case of positive signal, we refer to [18].

4 Conclusions

Phase I experiments will measure the parameters leading the oscillations at the atmospheric scale with unprecedented precision. They will fix the $\sin^2 2\theta_{23}$ and $|\Delta m_{31}^2|$ terms at the 1% level and observe a clear oscillation patterns in ν_μ disappearance mode. Moreover, they can test the subdominant $\nu_\mu \rightarrow \nu_e$ transition improving significantly the present knowledge of θ_{13} . On the other hand, the actual sensitivity to $\sin^2 2\theta_{13}$ is strongly deteriorated by the present ignorance on the CP violating phase and the sign of Δm_{31}^2 . In Sec. 3 it has been shown that, in case of null result, the improvements in the exclusion limits for $\sin^2 2\theta_{13}$ will be marginal with respect to long baseline experiments like ICARUS and OPERA ($0.03 \rightarrow 0.015$) at $\alpha \simeq 0.02$ and negligible for higher values of α . On the other hand, a high solar scale ($\alpha > 0.02$) enhances significantly the capability of Superbeam and Neutrino Factory to access CP violation even for values of $\sin^2 2\theta_{13} \sim \mathcal{O}(10^{-3} \div 10^{-4})$. Hence, a null result at Phase I will not constrain in a significant way the physics reach of SB/NF. Clearly, it is impossible to tune a Phase I experiment to reach simultaneously a high $\sin^2 2\theta_{13}$ sensitivity (setups “ancillary” to Phase II) and a high sensitivity to the CP phase and the mass hierarchy (setups with high “PMNS reach”). At present we do not know if JHF-SK and NuMI Off-Axis belong to the former or latter category, due to the large uncertainty on α . Anyway, a real Phase I experiment (or cluster of experiments) performing a “pure” $\sin^2 2\theta_{13}$ along the line proposed by the authors of [17, 18, 19] would be highly advisable to firmly ground the SB/NF physics programme.

Acknowledgements

We thank A. Donini, M. Lindner, M. Mezzetto and P. Strolin for discussions and careful reading of the manuscript. We are indebted to D. Meloni for providing us with the

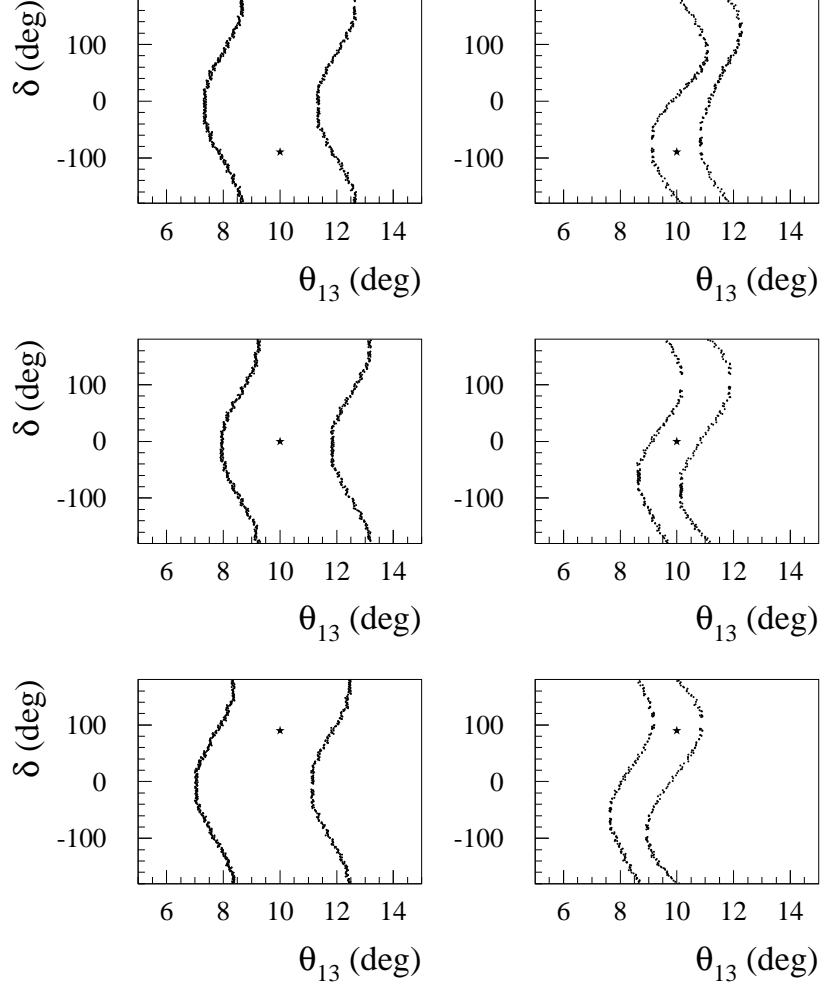


Figure 8: Left plots: 90% CL allowed region after 5 years of CNGS data taking for $\theta_{13} = 10^\circ$, normal hierarchy and $\delta = -90^\circ$ (upper), $\delta = 0^\circ$ (middle), $\delta = 90^\circ$ (lower plot). The plots on the right show the corresponding regions obtained combining CNGS data with a 5-year run of JHF-SK. The stars indicate the true value of θ_{13} and δ .

three family oscillation code and to P. Huber for useful remarks on Eq. 2.

References

- [1] Y. Fukuda *et al.* [Super-Kamiokande Coll.], Phys. Rev. Lett. **81**, 1562 (1998)
M. Ambrosio *et al.* [MACRO Coll.], Phys. Lett. **B517** (2001) 59
B.T. Cleveland *et al.*, Astrophys. J. **496**, 505 (1998)
J.N. Abdurashitov *et al.* [SAGE Coll.], Phys. Rev. **C60**, 055801 (1999)
W. Hampel *et al.* [GALLEX Coll.], Phys. Lett. **B447**, 127 (1999)
S. Fukuda *et al.* [Super-Kamiokande Coll.], Phys. Rev. Lett. **86**, 5651 (2001)
Q.R. Ahmad *et al.* [SNO Coll.], Phys. Rev. Lett. **87**, 071301 (2001).
- [2] M.H. Ahn *et al.* [K2K Coll.], Phys. Rev. Lett. **90** (2003) 041801.
- [3] K. Eguchi *et al.* [KamLAND Coll.], Phys. Rev. Lett. **90** (2003) 021802.
- [4] G.L. Fogli *et al.*, Phys. Rev. **D67** (2003) 073002
M. Maltoni, T. Schwetz and J. W. Valle, hep-ph/0212129.
- [5] E. Church *et al.*, LA-UR-98-352, Fermilab experiment 898.
- [6] E. Ables *et al.* [MINOS Coll.], FERMILAB-PROPOSAL-P-875
The MINOS detectors Technical Design Report, NuMI-L-337, October 1998.
- [7] F. Arneodo *et al.* [ICARUS Coll.], ICARUS-TM/2001-08 LNGS-EXP 13/89
add.2/01.
- [8] M. Guler *et al.* [OPERA Coll.], CERN-SPSC-2000-028.
- [9] Z. Maki, M. Nakagawa and S. Sakata, Prog. Theor. Phys. **28** (1962) 870
B. Pontecorvo, Sov. Phys. JETP **26** (1968) 984.
- [10] See e.g. [31] and references therein.
- [11] C. Jarlskog, Phys. Rev. Lett. **55** (1985) 1039.
- [12] K. Hagiwara *et al.*, Phys. Rev. **D66** (2002) 010001.
- [13] M. Apollonio *et al.* [CHOOZ Coll.], Eur. Phys. J. **C27** (2003) 331.
- [14] F. Boehm *et al.* [PALO VERDE Coll.], Phys. Rev. **D64** (2001) 112001.
- [15] Y. Itow *et al.*, KEK-REPORT-2001-4, hep-ex/0106019.
- [16] D. Ayres *et al.*, hep-ex/0210005.
- [17] P. Huber, M. Lindner and W. Winter, Nucl. Phys. **B654** (2003) 3.

- [18] T. Kajita, H. Minakata and H. Nunokawa, Phys. Lett. **B528** (2002) 245.
- [19] H. Minakata et al., hep-ph/0211111.
- [20] A. Cervera et al., Nucl. Phys. **B579** (2000) 17, erratum ibid. Nucl. Phys. **B593** (2001) 731.
- [21] M. Freund, Phys. Rev. **D64** (2001) 053003.
- [22] V. Barger, D. Marfatia and K. Whisnant, Phys. Rev. **D65** (2002) 073023.
- [23] J. Burguet-Castell *et al.*, Nucl. Phys. **B608** (2001) 301.
- [24] J. Burguet-Castell *et al.*, Nucl. Phys. **B646** (2002) 301.
V. Barger, D. Marfatia and K. Whisnant, Phys. Rev. **D66** (2002) 053007.
- [25] A. Donini, D. Meloni and P. Migliozi, Nucl. Phys. **B646** (2002) 321.
- [26] M. Freund, P. Huber and M. Lindner, Nucl. Phys. **B615** (2001) 331
M. Diwan *et al.*, BNL-69395, hep-ex/0211001.
- [27] M. Komatsu, P. Migliozi and F. Terranova, J. Phys. **G29** (2003) 443.
- [28] M. Diwan et al., NuMI-NOTE-SIM-0714.
- [29] T. Nakaya, Talk given at the “XXth International Conference on Neutrino Physics and Astrophysics”, Munich, Germany, May 25-30, 2002.
- [30] S.M. Bilenky, D. Nicolo and S.T. Petcov, Phys. Lett. **B538** (2002) 77.
- [31] P. Huber, M. Lindner and W. Winter, Nucl. Phys. **B645** (2002) 3.